Journal of Solid State Chemistry **142,** 368–373 (1999)
Article ID jssc.1998.8050, available online at http://www.idealibrary.com on IDEAL®

Grafting Mechanism of Electrochromic PAA–WO_3 Composite Film

J.-H. Choy,*,[1] Y.-I. Kim,* B.-W. Kim,* G. Campet,† J. Portier,† and P. V. Huong‡

*Department of Chemistry and Center for Molecular Catalysis, Seoul National University, Seoul 151-742, Korea; †Institut de Chimie de la Matière Condensée, Université de Bordeaux 1, Avenue du Dr Schweizer, Pessac 33608, France; and ‡Laboratoire de Spectroscopie Moléculaire et Cristalline, URA 124 CNRS, Université de Bordeaux 1, 351 Cours Libération, Talence 33405, France

Received March 2, 1998; in revised form September 29, 1998; accepted October 6, 1998

A micro-Raman spectroscopic study has been carried out to investigate the electrochromic process in a porous and nanocrystalline tungsten oxide film. The film was prepared by dipping the tin-doped indium oxide glass into an aqueous mixture solution of PAA (polyacrylic acid) and WO_3–NH_4OH. After heating at low temperature, around 100°C, the film was treated in 1 N HCl in order to achieve polycondensation, where the ammonium ion was replaced with a proton. In the micro-Raman spectra for the bleached and colored PAA–WO_3 films, it was evident that the coloration accompanies a peak reduction at $\sim 960\ cm^{-1}$ and a peak enhancement at $\sim 810\ cm^{-1}$. Based upon the present Raman observation, we can confirm that the electrochromism of the nanocrystalline tungsten oxide is dominated by the grafting process, i.e., the surface modification of $-W^{VI}=O$ bonds into $-W^{V}=O^{(1-\delta)+}—M^{\delta+}$ (M = H, Li) ones. © 1999 Academic Press

INTRODUCTION

Electrochromism refers to the reversible color change of electrochromic materials, which is triggered by the applied electric current or potential. With a view to the application to information display, light shutter, smart window, variable reflectance mirror, etc., various electrochromic materials have been explored (1, 2). Tungsten oxide has been the most extensively studied because of its deep and stable color change during the reversible "redox" reaction of cation (H^+, Li^+, Na^+, or K^+) insertion/deinsertion. It is generally understood that the electrochromic function of WO_3 film (response time, durability, coloration efficiency, etc.) depends on its microstructure (2), and that the porous and amorphous films can exhibit a better electrochromic property of fast and strong coloration (2). We have recently developed a new solution route to prepare uniform and hybrid tungsten oxide film by successive coatings of polyacrylic acid (PAA) and WO_3 solutions (3–6). From transmission electron microscopy, the resulting PAA–WO_3 composite films were found to be nanocrystalline, with grain size ~ 4 nm (5), so that they can exhibit an efficient coloration property by H^+/Li^+ injection.

As the mechanism for the cation intercalation into such nanocrystalline oxides, some of us proposed the electrochemical grafting of the ionic H^+/Li^+ species onto the crystallite surfaces (7, 8). This mechanism has not yet been clearly verified, and the grafting process should be investigated using a molecular spectroscopy such as micro-Raman which can provide detailed information on the structural changes (9, 10) from the viewpoint of chemical bonding. In this work, a more simplified method is presented to make the porous and nanocrystalline PAA–WO_3 composite film, and micro-Raman spectroscopy is utilized to probe the cation insertion/deinsertion reaction, via the narrow and intense vibrational lines of the W–O frame with a precise spatial resolution (1 μm^3).

EXPERIMENTAL

For sample preparation and analyses, chemical reagents of WO_3 (Aldrich, 99 + %), PAA (Aldrich, $Mv \sim 450{,}000$), H_2WO_4 (Aldrich, 99%), and $(NH_4)_2WO_4$ (Aldrich, 99.99%) were used without any further purification.

In order to obtain a homogeneous PAA solution, 12.5 g of PAA was dissolved in 100 ml of deionized water by stirring for 24 h at room temperature. Tungsten oxide basic solution was prepared as follows. First, 7 g of WO_3 was added to 40 ml of 15% NH_4OH solution. After stirring for 4 h at 100°C, 60 ml of deionized water was added, stirred for 24 h at room temperature and filtered. The dip-coating solution was prepared by mixing tungsten oxide basic solution (50 ml) and PAA solution (12.5 g).

The tin-doped indium oxide (ITO) glass (Samsung Corning, 15 Ω/□) substrate was dipped into the mixed aqueous solution and withdrawn vertically at a speed of 12 cm/min. After heating at 100°C for 10 min, the film was treated in 1 N HCl solution for 3 min to achieve polycondensation by replacing the ammonium ion with a proton.

[1] To whom correspondence should be addressed. Fax: +82-2-872-9864. E-mail: jhchoy@plaza.snu.ac.kr.

0022-4596/99 $30.00

In order to investigate the tungstate structure of the PAA–WO_3 nanocrystalline film, larger crystallites of tungstate were prepared separately, in a manner similar to that used for making the composite film. The above WO_3–NH_4OH solution was dried in an ambient atmosphere, and the resulting powder (denoted hereafter as WD) was treated in 1 N HCl for one day, washed with deionized water, and dried (denoted hereafter as WDH). For the Raman study on the WDH grain, before and after the electrochemical H^+ insertion, WD powder was dispersed on the as-dipped PAA–WO_3 layer (on ITO glass) and transformed to WDH by the chemical treatment in 1 N HCl.

The PAA–WO_3 film thickness of $\sim 0.65\,\mu m$ could be measured by scanning electron microscopy (JEOL, JSM 840-A), and the area density of W was determined to be $0.13_4\,mg/cm^2$ (corresponding to $\sim 0.73\,\mu mol/cm^2$), using the inductively coupled plasma spectrometry. The XRD (X-ray diffraction) patterns were obtained by Philips FR590 X-ray diffractometer (Cu$K\alpha$, 20 kV/30 mA) for the powder samples, and by MAC Science MXP-3VA diffractometer (Cu$K\alpha$, 40 kV/40 mA, with the grazing angle of 0.5°) for the films.

In situ opto-electrochemical measurements were carried out using a potentiostat/galvanostat (Radiometer Copenhagen, PGP 201) and a specially designed visible apparatus. Transmittance (T%) of the film was monitored at the fixed wavelength of 550 nm, during the cyclic voltammetric or chronopotentiometric operations, where the standard three-electrode cell was used. The electrolyte was 10 wt% $Li(CF_3SO_2)_2N$ in 1,3-EtMeIm$(CF_3SO_2)_2N$, and the Ag/AgCl and Pt wire were used as reference and counter electrodes, respectively.

The micro-Raman measurements with a spatial resolution (11–13) of $1\,\mu m^3$ were performed with a LABRAM spectrometer (Jobin Yvon-Spex-Dilor) using an Ar ion laser (Spectra Physics) emitting at 514.5 nm. The optimum spectra could be obtained by adjusting the laser power (0.5 to 5 mW) and the data acquisition time (10 to 1500 s).

RESULTS AND DISCUSSION

Film Characterizations

Figure 1 shows the XRD patterns of the WDH, H_2WO_4 powders, and the PAA–WO_3 composite films as prepared and chemically treated in 1 N HCl. In case of the as-prepared film, a broad peak appeared at $2\theta = 10°$, which disappears after the treatment in HCl. Although the film samples, in both states, are X-ray amorphous, this is surely due to the limited thickness and the crystallite size of the film. Therefore, we have also investigated the XRD pattern of WDH, which was prepared by the procedure analogous to that for the PAA–WO_3 film, in comparison with those of several reference compounds. As can be seen in Fig. 1, the WDH powder exhibits an XRD pattern quite similar to that of H_2WO_4, except for the relative peak intensities between two peaks at $2\theta = 16.7°$ ([020]) and 25.8° ([111]), which can be explained simply by the orientation effect (14). Based on these findings, we could expect that the chemically treated PAA–WO_3 film has a crystal structure similar to that of the WDH powder and also to that of the H_2WO_4.

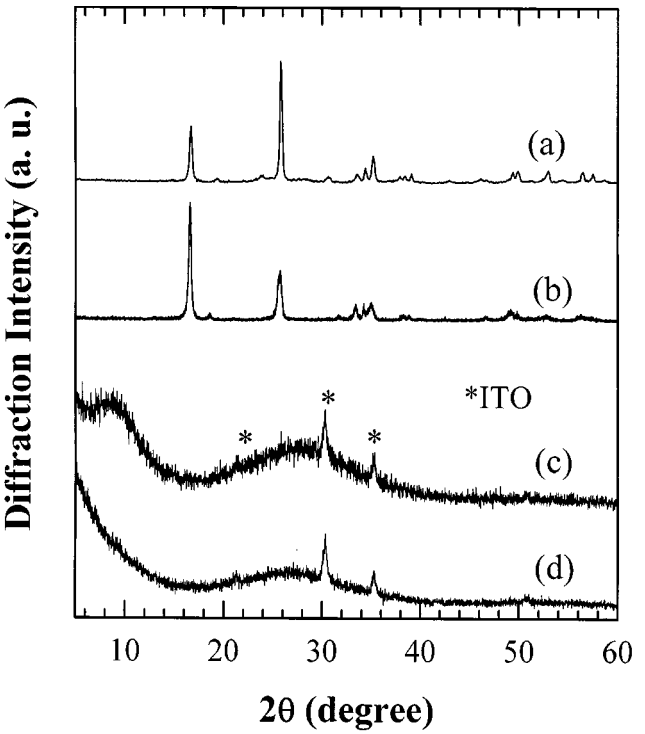

FIG. 1. XRD patterns for (a) H_2WO_4, (b) WDH powder, (c) as-prepared PAA–WO_3 film, and (d) chemically treated PAA–WO_3 film.

The electrochromic property of the PAA–WO_3 composite film is represented in Figs. 2 and 3. During the cyclic voltammetry at the potential range of -0.8–$+0.5$ V (vs Ag/AgCl), the film exhibits a well-known redox behavior of $W^{VI \leftrightarrow V}$, which accompanies a reversible color change between the transparent colorless and the dark blue ($\Delta T\% \approx 80$). Also by the galvanostatic reduction ($j = 50\,\mu A/cm^2$), the transmittance of the film could be controlled (Fig. 3). By the Li^+ insertion with $12.5\,mC/cm^2$, a remarkable blue color was attained with the optical density (ΔOD) of 0.55, which corresponds to the coloration efficiency (η) of $\sim 44\,cm^2/C$. As can be seen in the potentiometric profile, the electrode potential (E) is maintained within the stable range of -0.5 V–$+2.3$ V vs Ag/AgCl.

Raman Analysis on the PAA–WO_3 Film

Several research groups have already reported the Raman and infrared (IR) spectroscopic studies (9, 15–17) on the electrochromic process of tungsten oxide film. By reviewing

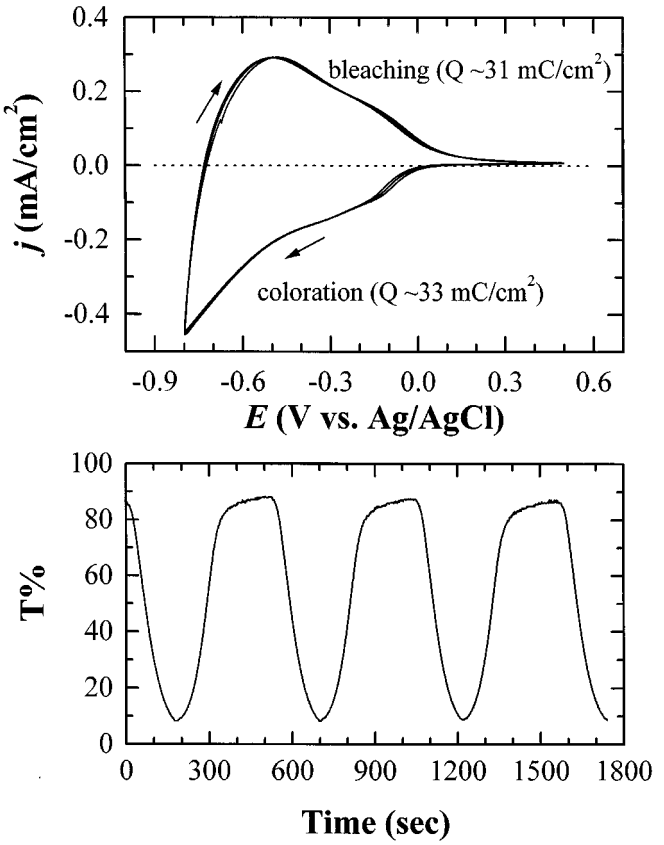

FIG. 2. (top) Cyclic voltammetry and (bottom) *in situ* optical measurement at $\lambda = 550$ nm for the chemically treated PAA–WO_3 composite film.

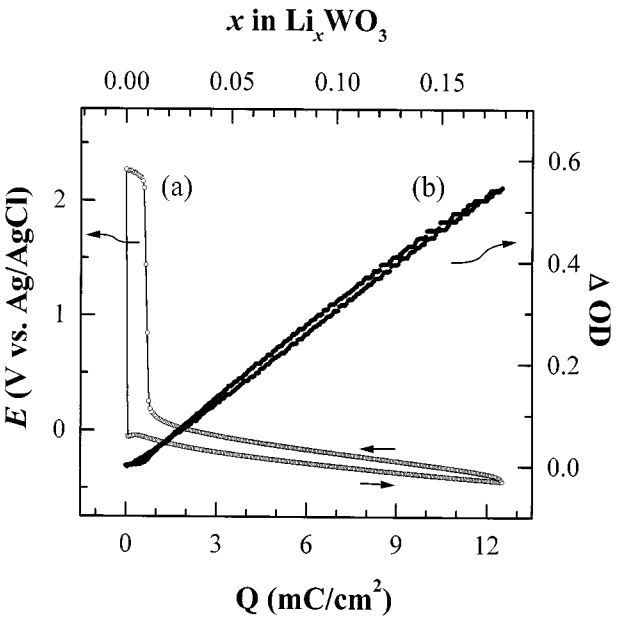

FIG. 3. (a) Chronopotentiometry ($j = 50\ \mu A/cm^2$, maximum $Q = 12.5\ mC/cm^2$) and (b) *in situ* optical density measurement at $\lambda = 550$ nm, for the chemically treated PAA–WO_3 composite film. The ΔOD is ~ 0.55 at $Q = 12.5\ mC/cm^2$.

those previous works, one can easily find out that their main interests were focused on the evolution of spectral features at ~ 950 and $\sim 800\ cm^{-1}$, which correspond to the ν(W=O) and ν(O–W–O) vibrational motions, respectively. Delichère *et al.* (9) and Paul *et al.* (15) observed, upon H^+/Li^+ injection (colorlation), an increase of the peak at $\sim 950\ cm^{-1}$ and a simultaneous depression at $\sim 800\ cm^{-1}$. Based on those results, they assumed that the inserted ions are bound to the oxygen in W–O–W chain, so that a W–O bond is broken and a W=O bond is formed instead. On the contrary. Otsuka *et al.* (16) and Habib *et al.* (17) showed that the coloration occurs with the enhancement of the Raman or IR signals at $\sim 950\ cm^{-1}$, and thereby demonstrated that the inserted cation incorporates at the $-$W=O site, transforming the terminal –W=O bond into the W–O–H(Li) one.

Seemingly, these results are contradictory, but it should be noted that the film used in each study was different, in the deposition method and condition. By using the lower energy and power for film fabrication, a less crystalline and defective tungsten oxide phase can be obtained, which abounds in the W=O bonds. The cation insertion into such an amorphous film would occur at the W=O terminal, since it is favored from the steric and electronic aspects. In the opposite case of crystalline WO_3, there are fewer W=O bonds, and it is expected that the W–O–W site should be significantly affected by cation insertion. Namely, the electrochromic reaction of the tungsten oxide film can occur with a different mechanism, depending upon its preparation condition and crystallinity.

In case of present PAA–WO_3 film, the electrochromic WO_3 grains are formed with crystallite size ~ 4 nm, as mentioned above. Therefore, we believe that it should be the most suitable system for the Raman study of electrochromic process in the nanocrystalline film with many W=O terminal bonds.

As shown in Fig. 4, where the micro-Raman spectra for WO_3, $(NH_4)_2WO_4$, H_2WO_4 chemicals, and WDH powder are presented, the overall spectral feature of WO_3 is similar to that of the monoclinic WO_3 (18). The strong peaks at 805 and 715 cm^{-1} are assigned as stretching vibrations of octahedral tungsten with neighboring oxygens [ν(O–W–O)], and those at 274 and 330 cm^{-1} are due to the bending vibration [δ(O–W–O)]. Other small peaks below 200 cm^{-1} result from the lattice modes of W–O–W network. The peaks observed for $(NH_4)_2WO_4$, around 1675 and 1418 cm^{-1} can be attributed to the vibrations of NH_4^+. However, the stretching vibrations of NH_4^+ appeared at a lower energy side than those of free NH_4^+ (19) due to the interaction between NH_4^+ and WO_4^{2-}. The characteristic frequencies of WO_4^{2-} in $(NH_4)_2WO_4$, occurring at 952, 875,

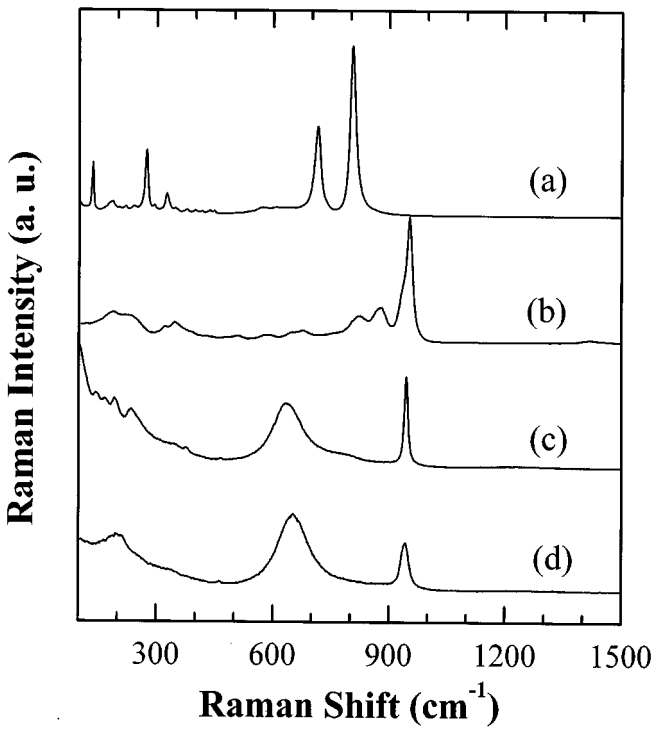

FIG. 4. Micro–Raman spectra for (a) WO_3, (b) $(NH_4)_2WO_4$, (c) H_2WO_4, and (d) WDH powder.

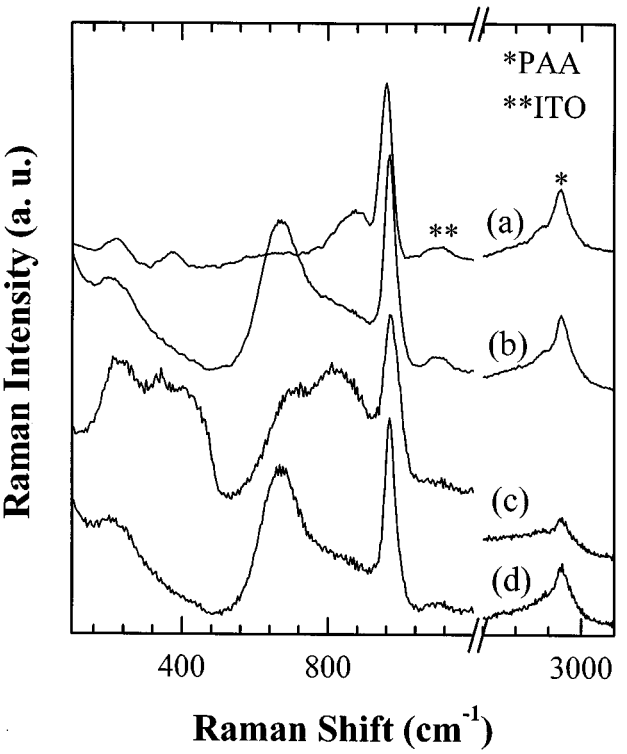

FIG. 5. Micro–Raman spectra of PAA–WO_3 composite films (a) as prepared, (b) after chemical treatment in HCl, (c) H^+ colored, and (d) bleached.

822, and 346 cm^{-1}, are shifted and split compared to those of tetrahedral WO_4^{2-} (18, 19), because the WO_4^{2-} in $(NH_4)_2WO_4$ is rather distorted.

In the case of H_2WO_4, a sharp peak at 945 cm^{-1} and a broad one at 633 cm^{-1} are observed, due to the stretching vibrations of terminal W=O (20) and the bulk O–W–O network, respectively. As shown in Fig. 4, the Raman spectrum of WDH represents overall similarities to that of H_2WO_4, revealing that the nonstoichiometric species of ammonium tungstate hydrates (WD) is turned into H_2WO_4 (at least partially) according to the following substitution reaction:

$$\underset{\text{WD}}{(NH_4)_2WO_4 \cdot yH_2O} + 2H^+ \rightarrow \underset{\text{WDH}}{H_2WO_4} + 2NH_4^+ + yH_2O$$

The effect of chemical treatment on the PAA–WO_3 composite film has also been examined by comparing micro-Raman spectra of the as-prepared (Fig. 5a) and chemically treated (Fig. 5b) films. The spectral feature of the as-prepared film is rather similar to that of $(NH_4)_2WO_4$ except for the peaks originating from ITO and PAA. After the chemical treatment, the characteristic peak of ammonium tungstate (at 875 cm^{-1}) disappears while an intense Raman peak appears at 672 cm^{-1}, which is attributed to a stretching mode of O–W–O lattice. This indicates that the ammonium ions in the film are surely replaced with protons and the –O–W–O– network is newly formed upon chemical treatment. In fact, the frequencies and relative intensities of main peaks of the chemically treated film (Fig. 5b) are consistent with those of tungstic acid (Fig. 4c), which clarifies that the nonstoichiometric ammonium tungstate hydrates in the as-prepared film are transformed to tungstic acid by the H^+ treatment.

The chemically treated glass which contains both WDH grain and PAA–WO_3 composite film showed good electrochromic property by H^+ insertion, not only in the film part but also in the grain. Because the finely grained WDH has been prepared under the samely mild condition (100°C) as the film, the grain surface of WDH can possess a large concentration of reaction sites for H^+ ion, as is for the film. Micro-Raman spectra of WDH grain, colored (Fig. 6b) and bleached (Fig. 6c) by electrochemical H^+ insertion/deinsertion, are represented, together with the spectrum of H^+ colored PAA–WO_3 film (Fig. 6a). The two spectra of Fig. 6a and 6b are nearly the same, which implies that the H^+ inserted amorphous tungstate in PAA–WO_3 medium has a structure similar to that of H^+ inserted WDH grain. A sharp and intense peak observed at 969 cm^{-1} accounts for the terminal –W=O bonds.

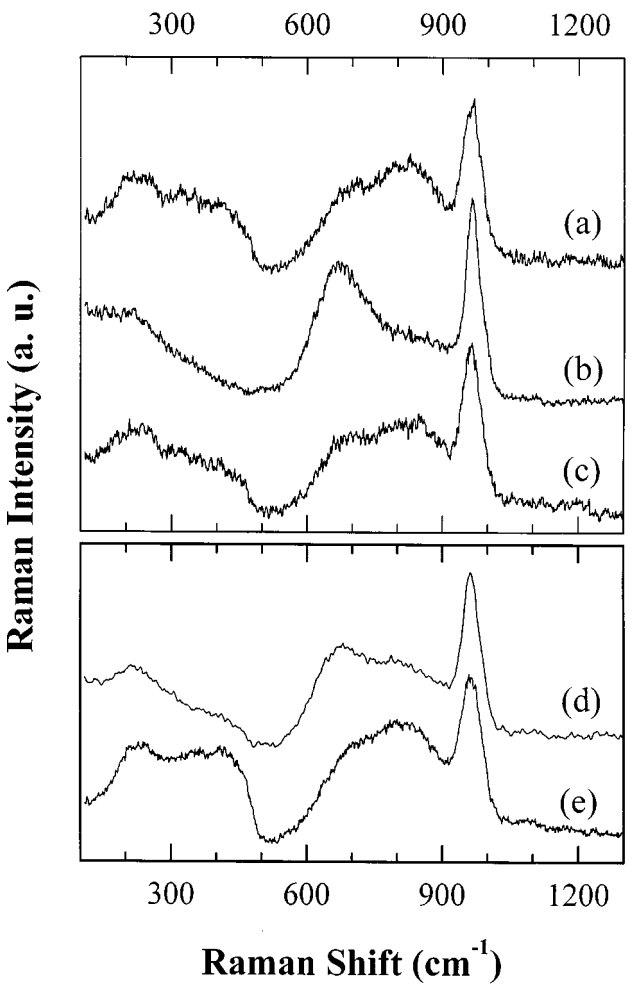

FIG. 6. (top) Micro–Raman spectra for the PAA–WO_3 film containing dispersed WDH grain, (a) H^+ colored film medium, (b) H^+ colored WDH grain, and (c) bleached WDH grain. (bottom) Micro–Raman spectra of PAA–WO_3 composite film, (d) bleached and (e) Li^+ colored with $Q = 15\ mC/cm^2$.

As already shown in Fig. 5, the micro-Raman spectrum of the H^+ colored film is somewhat different from that of the bleached one. A remarkable change due to H^+ insertion is the enhancement of the peak at 811 cm^{-1} (O–W–O) and the decrease of peak intensity at 969 and 672 cm^{-1} which are attributed to the vibrations of ν(W=O) and ν(O–W–O), respectively. We believe that such a change in the Raman spectra results from the above-mentioned electrochemical grafting process of the H^+ species onto the crystallite surface of the nanocrystalline WDH, in which the terminal –W=O bonds transform into $-W^V = O^{(1-\delta)+}-H^{\delta+}$ ones. Therefore the spectral change at 811 cm^{-1} accounts for the reduced double bond character of the $W^V=O^{(1-\delta)+}$. In addition, the suppressed Raman feature at 672–680 cm^{-1} implies that the grafting process gives rise to a considerable perturbation on the internal O–W–O lattice of the nanocrystalline tungstate. The small changes below 400 cm^{-1}, which indicate the change of O–W–O bending vibration, are also due to the modification of internal lattice by proton insertion.

Similar changes in micro–Raman spectra were observed also for Li^+ insertion/disinsertion, as displayed in Figs. 6d and 6e. After Li^+ insertion, the Raman intensity decreases at 680 cm^{-1} and increases at 800 cm^{-1}, which can be explained in the same manner as in H^+ insertion/deinsertion. In this case, the terminal bond should be transformed to $-W^V=O^{(1-\delta)+}-Li^{\delta+}$, by the grafting process. It can be noted that the structural changes induced by H^+ (Li^+) insertion/deinsertion are reversible and reproducible.

A possible mechanism for the reversible electrochromic effect of the PAA–WO_3 films can be proposed as follows. The porous and nanocrystalline structure of the film favors the formation of W=O terminal bonds at the crystallite surface. These "structural defects" which create deep subband gap energy state inside the band energy gap, act as reversible grafting sites for M^+ ions (M = H or Li). The blue coloration observed for the H^+/Li^+ grafted films must be associated with an absorption of visible light and the concurrent electron excitation from W^V ($5d^1$) subband gap energy states to the conduction band. The absorption process can be depicted as follows:

$$W^V\ (5d^1) \xrightarrow{h\nu\,(\text{visible})} W^{VI}(5d^0) + e^-$$

deep electron donor center	"ionized" donor center	in the conduction band of W^{VI} ($5d^0$) parentage

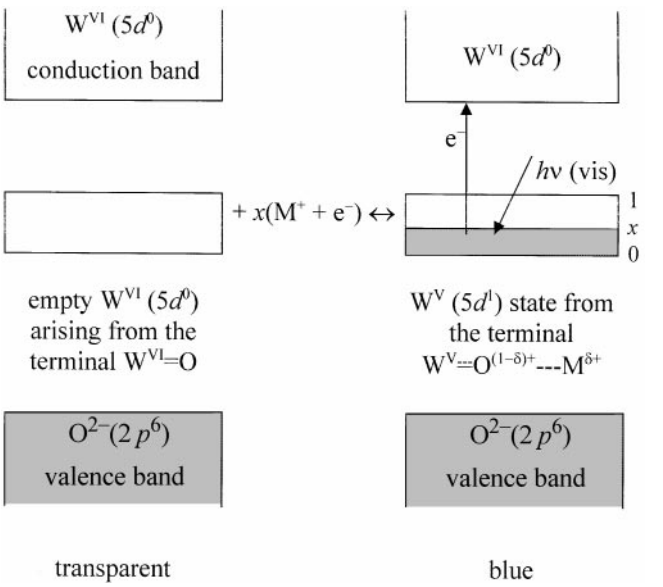

FIG. 7. Simplified band energy scheme illustrating the visible light absorption process in the grafted film.

The W^V ($5d^1$) state, which is just below the conduction band of W^{VI} ($5d^0 : t_{2g}$) parentage, arises from the $-W^V=O^{(1-\delta)+}—M^{\delta+}$ bond. This is illustrated in Fig. 7, using a simplified band energy diagram (with the approximation of the "ionic model").

CONCLUSION

Tungsten oxide–based films have been prepared by dip coating, using an aqueous solution of PAA and WO_3–NH_4OH mixed solution. The ammonium ions in the as-prepared film could be replaced by protons through chemical treatment in 1 N HCl solution, and the resulting PAA–WO_3 film exhibited good electrochromic properties by reversible cation ($M^+ = H^+$, Li^+) insertion. From the XRD and micro-Raman spectroscopy studies, the tungsten species in the PAA–WO_3 film turned out to have almost the same crystal structure as H_2WO_4. The Raman observation indicated that the inserted M^+ ion combines with terminal –W=O to make a new $-W^V=O^{(1-\delta)+}—M^{\delta+}$ bond, through the grafting process. This allowed us to propose a mechanism explaining the reversible electrochromic effect observed for the films. It can be inferred that a rather similar grafting mechanism occurs for all nanocrystalline materials having high electrochemically active surface area.

ACKNOWLEDGMENTS

This work was in part supported by the Korea Science and Engineering Foundation (KOSEF) through the Center for Molecular Catalysis (CMC), and by the Korean Ministry of Trade and Industry, based on the Korea–France international collaboration program.

REFERENCES

1. P. M. S. Monk, R. J. Mortimer, and D. R. Rosseinsky, "Electrochromism, Fundamental and Applications." VCH, New York, 1995.
2. C. G. Granqvist, "Handbook of Inorganic Electrochromic Materials." Elsevier, Amsterdam, 1995 (and references therein).
3. N.-G. Park, B.-W. Kim, A. Poquet, G. Campet, J. Portier, J.-H. Choy, and Y.-I. Kim, *Active Passive Elec. Comp.* **20,** 125 (1998).
4. J.-H. Choy, Y.-I. Kim, S.-H. Choy, N.-G. Park, G. Campet, and J. Portier, "Electrochromic Materials and Their Applications III" (K.-C. Ho, C. B. Greenberg, and D. M. MacArthur, Eds.), p. 303. Electrochemical Society, Pennington, ECS-PV 96–24, 1997.
5. J.-H. Choy, B.-W. Kim, Y.-I. Kim, G. Campet, J. Portier, and J. C. Grenier, manuscript in preparation.
6. N.-G. Park, A. Poquet, G. Campet, J. Portier, J.-H. Choy, Y.-I. Kim, D. Camino, and J. Salardenne, *Active Passive Elec. Comp.* **20,** 201 (1998).
7. G. Campet, S. J. Wen, S. D. Han, M. C. R. Sharstry, J. Portier, C. Guizard, L. Cot, Y. Xu, and J. Salardenne, *Mater. Sci. Eng. B* **18,** 201 (1993).
8. S. D. Han, N. Treuil, and G. Campet, *Active Passive Elec. Comp.* **16,** 13 (1994).
9. P. Delichere, P. Falaras, M. Froment, A. Hugot-Le Goff, and B. Aguis, *Thin Solid Films* **161,** 35 (1988).
10. M. Pham Thi and G. Velasco, *Rev. Chim. Minér.* **22,** 195 (1985).
11. P. V. Huong, "Analytical Raman Spectroscopy" (J. Grasselli and B. Bulkin Eds.), p. 397. Wiley, New York, 1991.
12. P. V. Huong, *Vib. Spec.* **11,** 17 (1996).
13. P. V. Huong, *Fresenius J. Anal. Chem.* **355,** 596 (1996).
14. J. Szymansky and A. Roberts, *Can. Mineral* **22,** 681 (1984).
15. J. L. Paul and J. C. Lassegues, *J. Solid State Chem.* **106,** 357 (1993).
16. T. Ohtsuka, N. Goto, and N. Sato, *J. Electroanal. Chem.* **287,** 249 (1990).
17. M. A. Habib and S. P. Maheswari, *J. Electrochem. Soc.* **138,** 2029 (1991).
18. M. F. Daniel, B. Desbat, and J. C. Lassegues, *J. Solid State Chem.* **67,** 235 (1987).
19. K. Nakamoto, "Infrared Spectra of Inorganic and Coordination Compounds," p. 107. Wiley, New York, 1963.
20. K. Nakamoto, "Infrared Spectra of Inorganic and Coordination Compounds," p. 103. Wiley, New York, 1963.